



A Journal of the Gesellschaft Deutscher Chemiker

# Angewandte Chemie

GDCh

International Edition

www.angewandte.org

## Accepted Article

**Title:** Scaffold design of trivalent chelator heads dictates high-affinity and stable His-tagged protein labeling in vitro and in cellulo

**Authors:** Karl Gatterdam, Eike F. Joest, Volker Gatterdam, and Robert Tampé

This manuscript has been accepted after peer review and appears as an Accepted Article online prior to editing, proofing, and formal publication of the final Version of Record (VoR). This work is currently citable by using the Digital Object Identifier (DOI) given below. The VoR will be published online in Early View as soon as possible and may be different to this Accepted Article as a result of editing. Readers should obtain the VoR from the journal website shown below when it is published to ensure accuracy of information. The authors are responsible for the content of this Accepted Article.

**To be cited as:** *Angew. Chem. Int. Ed.* 10.1002/anie.201802746  
*Angew. Chem.* 10.1002/ange.201802746

**Link to VoR:** <http://dx.doi.org/10.1002/anie.201802746>  
<http://dx.doi.org/10.1002/ange.201802746>

## COMMUNICATION

# Scaffold design of trivalent chelator heads dictates high-affinity and stable His-tagged protein labeling *in vitro* and *in cellulo*

Karl Gatterdam<sup>#</sup>, Eike F. Joest<sup>#</sup>, Volker Gatterdam, and Robert Tampé<sup>\*</sup><sup>#</sup>These authors contributed equally to this work.

**Abstract:** Small chemical/biological interaction pairs are at the forefront in tracing proteins' function and interaction at high signal-to-background ratio in cellular pathways. Pharma ventures have eager plans to develop *tris*NTA probes for *in vitro* and *in vivo* screening of His-tagged protein targets. However, the optimal design of scaffold, linker, and chelator head yet deserves systematic investigations to achieve highest affinity and kinetic stability for *in vitro* and especially cell applications. In this study, we report on a library of *N*-nitritriacetic acid (NTA) based multivalent chelator heads (MCHs) built up on linear, cyclic, and dendritic scaffolds and contrast these with regard to their binding affinity and stability for labeling of cellular His-tagged proteins. Furthermore, we assign a new approach for tracing cellular target proteins at picomolar probe concentrations in cells. Finally, we describe fundamental differences between the MCH scaffold and define a cyclic *tris*NTA chelator, which displays the highest affinity and kinetic stability of all reversible, low-molecular weight interaction pairs.

Decoding of protein tracks and interactions is essential towards a system-based understanding of biological processes as well as their dysregulation in diseases<sup>[1]</sup>. Generic tools are eagerly awaited to trace proteins by small chemical probes at high spatiotemporal resolution<sup>[2]</sup>. Protein labeling can be realized by either covalent bond formation, enzyme or affinity mediated attachment of certain precursors<sup>[3]</sup>. These methods offer versatile ways to analyze the activity, conformational states, the cellular localization, and interactions of the target protein.

The metal chelating *N*-nitritriacetic acid (NTA) and the oligohistidine-tag (His-tag) constitute a well-established interaction pair, which has first been described in immobilized metal ion affinity chromatography (IMAC)<sup>[4]</sup>. Specific binding is based on the formation of an octahedral complex of bivalent metal ions, such as Ni(II) or Co(II), with histidines (Figure 1e). The interaction is reversible and can be released by competition with histidine or imidazole. So far, the His-tag is the smallest and most commonly used affinity tag in life sciences, making it an attractive target for site-specific protein labeling and *in vitro* or *in vivo* screening approaches. Initial attempts of His-tag labeling utilized Ni-NTA modified dyes<sup>[5]</sup>. However, the low affinity ( $K_D \approx 10 \mu\text{M}$ ) and the fast off-rate ( $k_a \approx 1/\text{s}$ ) resulted in a very transient labeling by the His-tag/Ni-NTA pair<sup>[5a,6]</sup>. To overcome this limitation, we introduced the concept of multivalent chelator heads (MCHs), exploiting a molecular avidity effect. The MCHs contain two to six NTA units leading to (sub-)nanomolar binding affinity towards a

histidine tag for site-specific labeling of targets even in a crowded cellular environment with low toxicity<sup>[6-7]</sup>. Therefore, the combination of high-affinity binding properties and an ultra-small, non-disturbing affinity tag of smaller than 1 kDa enable (i) protein labeling with organic dyes<sup>[8]</sup>, quantum dots<sup>[9]</sup>, and streptavidin<sup>[10]</sup>, (ii) protein tethering to membranes<sup>[11]</sup>, liposomes<sup>[12]</sup>, glass surfaces<sup>[13]</sup>, gold interfaces<sup>[7a,14]</sup>, and nanoparticles<sup>[15]</sup>, (iii) guided high-affinity protein *trans*-splicing and 'traceless' labeling<sup>[16]</sup>, as well as (iv) stochastic sensing of single molecules in nanopores<sup>[17]</sup>, single-molecule tracking<sup>[18]</sup>, or super-resolution microscopy even in living cells<sup>[7b,19]</sup>. However, the overwhelming contingences connecting the NTA groups led to an inscrutable offer of MCH probes, e.g. even sharing the same nomination, despite a fundamentally different chemical structure.

Here, we disclose substantial differences between cyclic, linear, and dendritic MCHs, underlining that the structural organization of the NTA elements is important for the high affinity and kinetic stability. Furthermore, we describe the fine-tuned optimization of trivalent chelator heads towards the highest affinity (*i.e.* lower probe concentration) and especially kinetic stability as well as specificity (lower background). As a final milestone, we determine which of all currently available MCH probes are optimal for life science applications.

We first focused on the flexibility of the NTA-linker arm and the rigidity of the cyclic scaffold. For that purpose, new cyclic cyclam-Asp-*tris*NTA (**2**) and cyclen-Glu-*tris*NTA (**3**) were compared with cyclam-Glu-*tris*NTA (**1**), linear *tris*NTA (**4**) and (**5**), dendritic NTA-Dab-*tris*NTA (**6**), and NTA-Orn-*tris*NTA (**7**) (Figure 1a). The synthesis of cyclam-Asp-*tris*NTA (**2**) and cyclen-Glu-*tris*NTA (**3**) is related to the one of cyclam-Glu-*tris*NTA (**1**)<sup>[6]</sup> (Figure S1). NTA-Orn-*tris*NTA (**7**) was synthesized as previously described<sup>[20]</sup>, while NTA-Dab-*tris*NTA (**6**) was obtained via a new synthesis route (Figure S2). Linear *tris*NTA (**4**) and (**5**) were synthesized as recently described<sup>[21]</sup> (Figure S3). To compare their kinetic and thermodynamic parameters ( $k_a$ ,  $k_d$ ,  $K_D$ ), all trivalent chelator heads were conjugated to biotin via a flexible spacer to allow a highly controlled immobilization for interaction analysis with His-tagged proteins using surface plasmon resonance (SPR). The MCHs were immobilized at the lowest possible surface density to exclude any bias by multivalency effect at the sensor interface. This important aspect is often neglected when multivalent compounds are analyzed at interfaces. Based on the maximum binding capacity of the neutravidin-functionalized SPR chip (300 resonance units (RU) for cyclam-Glu-*tris*NTA (**1**)), we ensured a very low immobilization density of 10 RU for all biotin-PEG<sub>4</sub>-*tris*NTA compounds. Utilizing the His<sub>6</sub>-tagged maltose-binding protein (MBP-H<sub>6</sub>), the kinetic and thermodynamic binding properties of all MCHs were compared by SPR spectroscopy (Figure 1b-d), resulting in binding affinities in the range of 10-60 nM. All data were corrected for unspecific binding and were fitted by a Langmuir 1:1 isotherm<sup>[22]</sup>.

K. Gatterdam, E. F. Joest, Dr. V. Gatterdam, Prof. Dr. R. Tampé  
Institute of Biochemistry, Biocenter, Goethe-University Frankfurt  
Max-von-Laue-Str. 9, 60438 Frankfurt/M (Germany)  
E-mail: tampe@em.uni-frankfurt.de  
Homepage: <http://www.biochemie.uni-frankfurt.de>

The German Research Foundation (GRK 1986, SFB 902, SFB 807)  
and the Volkswagen Foundation (Az. 91 067) supported this work.

## COMMUNICATION

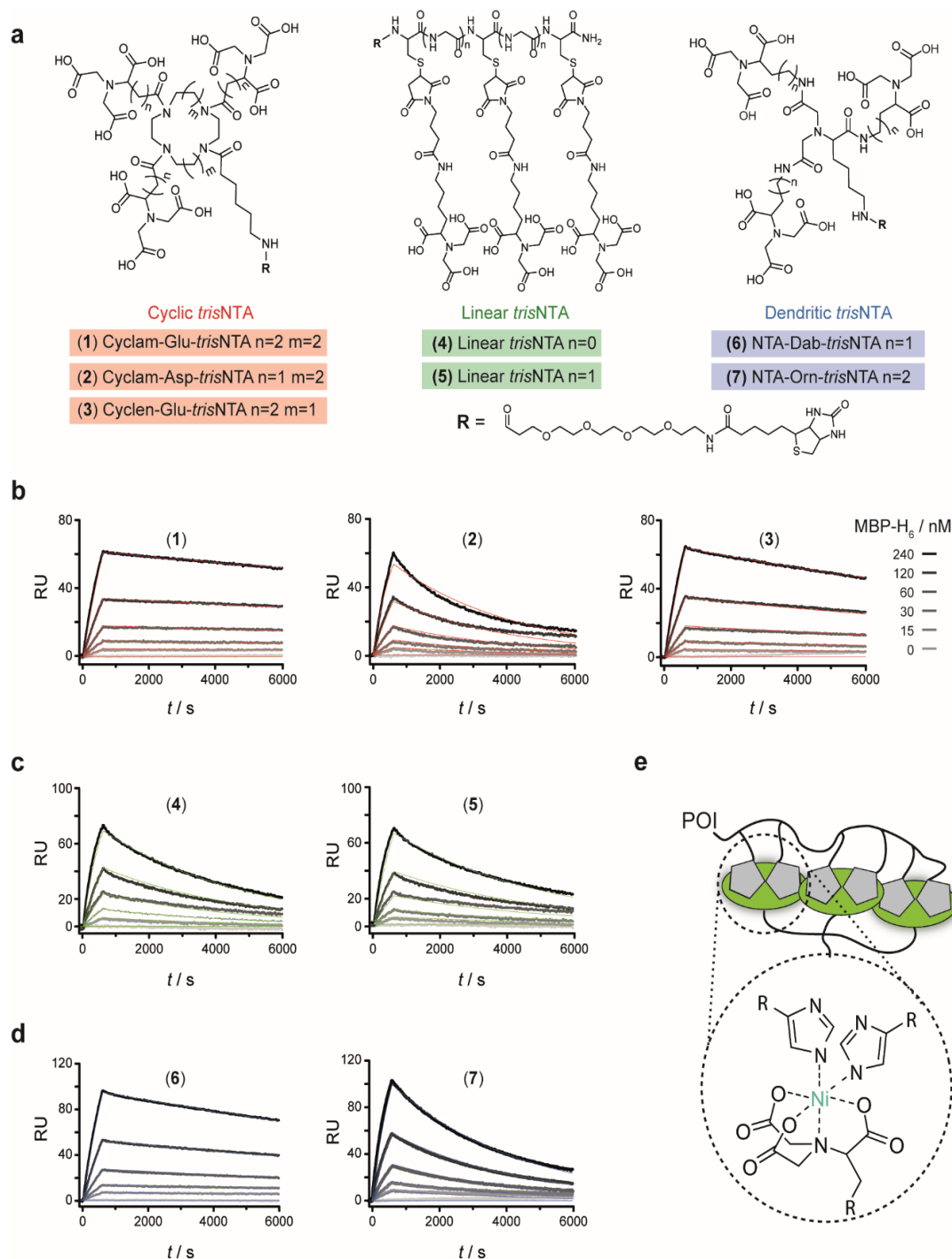


**Figure 1.** a) Chemical structures of trivalent chelator heads. The flexibility of the linker arms and the rigidity of the cyclic scaffold were fine-tuned, leading to cyclam-Asp-trisNTA (2) and cyclen-Glu-trisNTA (3), which were compared to the trivalent MCHs cyclam-Glu-trisNTA (1), linear trisNTA (4) and (5), NTA-Dab-trisNTA (6), and NTA-Orn-trisNTA (7). For surface immobilization, a biotin-PEG<sub>4</sub> linker of ~20 Å was introduced. b-d) Association and dissociation kinetics of MCHs with MBP-H<sub>6</sub>. Sensorgrams at different concentrations of MBP-H<sub>6</sub> binding to Ni(II)-loaded b) cyclam-Glu-trisNTA (1), cyclam-Asp-trisNTA (2), and cyclen-Glu-trisNTA (3), c) linear trisNTAs (4) and (5), d) NTA-Dab-trisNTA (6) and NTA-Orn-trisNTA (7). Data were fitted by a Langmuir 1:1 isotherm. e) Schematic illustration of the high-affinity His<sub>6</sub>-tag/trisNTA interaction pair. POI: protein of interest.

The respective kinetic parameters are summarized in Table 1. A full dataset is given in Table S2. Interestingly, the reduced NTA linker length of cyclam-Asp-trisNTA (2) and decreased flexibility of the cyclic scaffold as in cyclen-Glu-trisNTA (3) did not improve binding affinity and complex stability. In contrast, the off rates of the linear and dendritic chelators are significantly different in

comparison to the cyclic chelator (1) and (3) (Table 1). Cyclam-Glu-trisNTA (1) displayed the highest affinity and stability of all trivalent NTA compounds and outperformed any linear or dendritic trisNTA. Notably, the scaffold and linker length as well as the structural arrangement (linear, cyclic, dendritic) have a significant impact on the affinity.

## COMMUNICATION

**Table 1.** Kinetic and thermodynamic parameters of Ni(II)-loaded MCHs coordinating His<sub>6</sub>-tagged MBP analyzed by SPR spectroscopy.

trivalent NTA	cyclic			linear		dendritic	
	(1)	(2)	(3)	(4)	(5)	(6)	(7)
$k_s$ ( $10^3 \text{ M}^{-1} \text{ s}^{-1}$ )	3.21 $\pm 0.01$	5.17 $\pm 0.04$	2.49 $\pm 0.01$	6.57 $\pm 0.03$	4.65 $\pm 0.04$	2.97 $\pm 0.01$	4.68 $\pm 0.02$
$k_d$ ( $10^6 \text{ s}^{-1}$ )	3.05 $\pm 0.01$	27.40 $\pm 0.05$	5.97 $\pm 0.02$	23.20 $\pm 0.04$	22.30 $\pm 0.04$	5.61 $\pm 0.01$	26.60 $\pm 0.03$
$K_D$ (nM)	9.51 $\pm 0.06$	53.10 $\pm 0.51$	24.00 $\pm 0.18$	35.40 $\pm 0.22$	48.00 $\pm 0.50$	18.90 $\pm 0.10$	57.00 $\pm 0.31$

The cyclam-Glu-*tris*NTA system (**1**) appears to be optimized with regard to binding affinity and stability. A further option to increase the binding affinity would be the expansion of the His-tag (e.g. ten or twelve consecutive histidines). For MBP-H<sub>10</sub> and MBP-H<sub>12</sub>, the  $K_D$  values obtained by SPR spectroscopy ranged from 0.5 to 4.0 nM (Figure S5 and S6). Noteworthy, SPR analyses with very slow dissociation rates are difficult. Therefore, the MCH/His-tag interaction was challenged by increasing concentrations of imidazole (10 mM and 30 mM), which displaces the histidines and hence weakens the MCH/His-tag interaction. The complex stability with MBP-H<sub>12</sub> was strongly increased for cyclam-Glu-*tris*NTA (**1**) and cyclen-Glu-*tris*NTA (**3**), highlighting the important role of the cyclic scaffold. For comparison, the dissociation phase of MBP-H<sub>12</sub> was normalized (Figure 2a-c) and the dissociation rates were displayed as half-life times (Figure 2d; see Figure S9 for full dataset; see Figure S7 and S8 for full dataset of MBP-H<sub>6</sub> and MBP-H<sub>10</sub>). In terms of the entropic freedom of the cyclic scaffold, we concluded that the differences of the cyclam (flexible) and the cyclen (more rigid) scaffold only have a minor influence on the binding stability. In contrast, the NTA-linker arm has a strong impact as illustrated by the comparison of (**1**), (**2**), and (**3**). The long glutamate based NTA-linker arm in (**1**) and (**3**) is crucial for a stable interaction. These results confirm the large difference in the kinetic stability of the different trivalent chelator compounds.

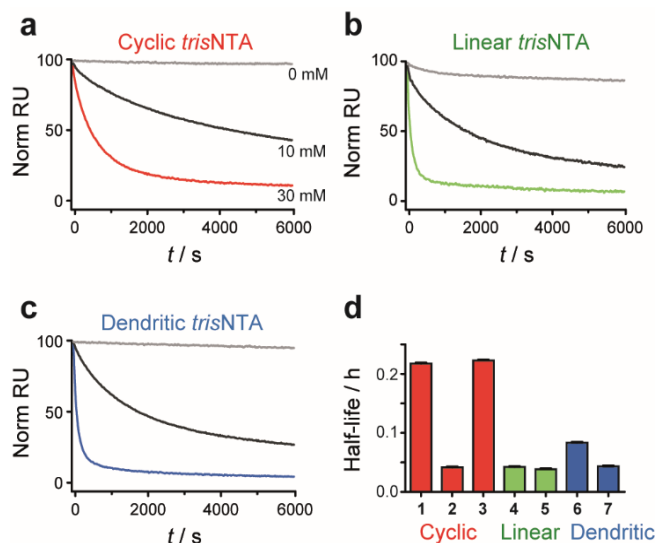


**Figure 2.** Kinetic stability of cyclic, linear, and dendritic *tris*NTA. After complex formation at 240 nM of MBP-H<sub>12</sub>, the dissociation phase was recorded in the presence of 0 mM (grey), 10 mM (black), and 30 mM of imidazole (colored) for Ni(II)-loaded a) cyclam-Glu-*tris*NTA (**1**), b) linear *tris*NTA (n=0) (**4**), and c) NTA-Orn-*tris*NTA (**7**). All data were fitted by a Langmuir 1:1 isotherm. d) Summary of complex stability of MCHs with 30 mM of imidazole as competitor. Data presented as means  $\pm$  s.d. of three independent experiments.

In conclusion, the cyclic trivalent chelator heads, cyclam- and cyclen-Glu-*tris*NTA (**1**) and (**3**), displayed a significantly higher kinetic stability compared to the linear or dendritic *tris*NTA, which is also reflected in the SPR data. Taking the results of all trivalent chelator heads into account, the cyclic scaffold as well as the linker of cyclam-Glu-*tris*NTA (**1**) (cyclic *tris*NTA) is optimized for high affinity and stable binding of His-tagged proteins.

To further clarify the observed differences in affinity and kinetic stability, we compared cyclic and linear *tris*NTA fluorophore conjugates as probes for intracellular protein labeling. To

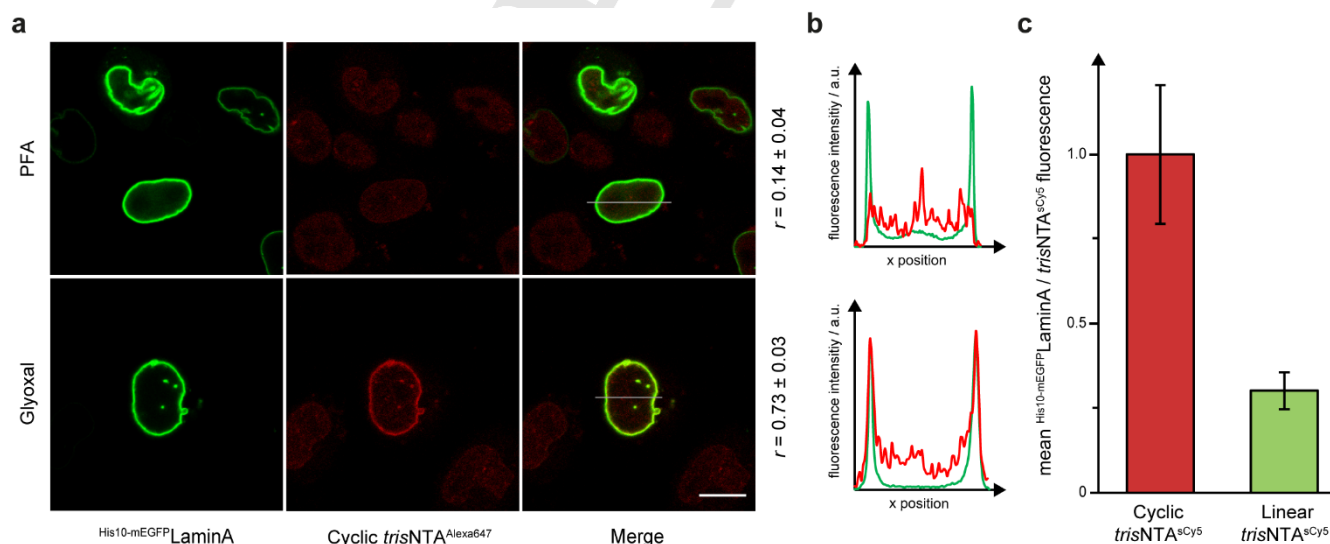


**Figure 3.** Labeling of intracellular His-tagged proteins by trivalent chelator probes. a) HeLa Kyoto cells were either treated by PFA or glyoxal and incubated with cyclic *tris*NTA<sup>Alexa647</sup> (**40**) (100 pM). Pearson's coefficients ( $r$ ) were determined by three distinct nuclei. Scale bar: 10  $\mu\text{m}$ . b) Corresponding intensity profiles of the indicated cross-sections. c) Labeling of transiently expressed, nuclear envelope located, His<sub>10</sub>-mEGFP<sup>LaminA</sup> by cyclic-*tris*NTA<sup>sCy5</sup> (**18**) or linear *tris*NTA<sup>sCy5</sup> (**34**) (100 pM each). Mean normalized labeling signal of glyoxal-fixed HeLa Kyoto cells (n = 10) is displayed. After labeling, cells were incubated with PBS containing 10 mM imidazole (3 h).

## COMMUNICATION

guarantee highest affinity, we additionally developed a novel MCH labeling protocol in fixed and permeabilized cells. By apprehending that consecutive histidines are prone to chemical modification during chemical fixation, we examined the direct labeling of intracellular His-tagged proteins by MCH fluorescent probes using glyoxal<sup>[23]</sup>. For comparison, we chemically arrested mammalian cells using conventional paraformaldehyde (PFA)<sup>[24]</sup> or glyoxal and imaged labeling using cyclic *tris*NTA coupled to the bright fluorophore Alexa647 (**40**) by confocal laser-scanning microscopy (CLSM). HeLa Kyoto cells transiently expressing His<sup>10</sup>-mEGFP<sup>LaminA</sup>, located at the nuclear envelope, revealed a strong and precise labeling at picomolar probe concentrations after glyoxal treatment, while PFA-treated cells showed no significant labeling under similar conditions (Figure 3a/b). We therefore hypothesized that the accessibility of the His-tag is largely improved using our advanced MCH labeling protocol. For a final statistic evaluation of the MCH scaffolds, we added 100 pM of either cyclic *tris*NTA<sup>sCy5</sup> (**18**) or linear *tris*NTA<sup>sCy5</sup> (**34**) probes to glyoxal-fixed HeLa Kyoto cells transiently expressing His<sup>10</sup>-mEGFP<sup>LaminA</sup>. Hereby, we mimicked SPR conditions and live cell environment by subsequently adding 10 mM imidazole (Figure S10). Afterwards, we imaged the cells by CLSM and analyzed the ratio of bound probe relative to the His<sup>10</sup>-mEGFP<sup>LaminA</sup> by densitometry (Figure 3c). Strikingly, we observed approximately 3-4 times more cyclic *tris*NTA<sup>sCy5</sup> (**18**) bound to His<sup>10</sup>-mEGFP<sup>LaminA</sup> in contrast to the linear *tris*NTA<sup>sCy5</sup> (**34**). We further delivered the cyclic *tris*NTA probe into the living cells and observed a highly specific labeling of His<sup>10</sup>-mEGFP<sup>LaminA</sup> (Figure S11).

In conclusion, we systematically worked out the importance of the scaffold design of trivalent MCHs affecting affinity and kinetic stability. Corresponding fundamental distinctions were visualized by a comprehensive SPR study of all MCHs, differing in their basic structural arrangement: linear, cyclic, dendritic. Furthermore, we directly contrasted cyclic *tris*NTA and linear *tris*NTA fluorophore conjugates for the tracing of intracellular His-tagged proteins. We therefore assigned a new glyoxal-fixation method for the first time to MCH labeling and thereby enabled the use of picomolar probe concentrations. Ultimately, we defined cyclic *tris*NTA as superior for in-vitro and cell applications, compared to the other described trivalent chelator heads. Thus, we suggest a detailed nomenclature for MCH molecules or to henceforth limit the simple term *tris*NTA to cyclam-Glu-*tris*NTA (cyclic *tris*NTA) in order to avoid obscurities. We hypothesize that, in combination with established MCH probe live-cell delivery techniques, like cell-squeezing or genetically encoded nanopores, these structural details and optimized trivalent MCHs can potentially enable chemically induced dimerization. Finally, these nanotools will open up new perspectives for ultra-small, non-disturbing and high-affinity labeling to gain deeper insights into dynamic cellular structures and processes.

## Acknowledgements

We thank Katrin Schanner for technical assistance, Drs. Ralph Wieneke, Markus Braner, and the entire lab for the helpful discussions.

**Keywords:** minimal tag • super-chelators • biosensors • protein labeling • target screening

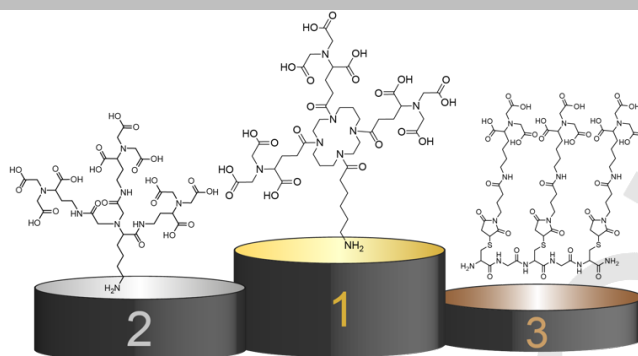
- [1] a) I. Chen, A. Y. Ting, *Curr. Opin. Biotechnol.* **2005**, *16*, 35-40; b) E. Toprak, P. R. Selvin, *Annu. Rev. Biophys. Biomol. Struct.* **2007**, *36*, 349-369; c) A. F. L. Schneider, C. P. R. Hackenberger, *Curr. Opin. Biotechnol.* **2017**, *48*, 61-68; d) M. J. Hinner, K. Johnsson, *Curr Opin Biotechnol* **2010**, *21*, 766-776; e) T. Schlichthaerle, M. T. Strauss, F. Schueder, J. B. Woehrstein, R. Jungmann, *Curr. Opin. Biotechnol.* **2016**, *39*, 41-47.
- [2] I. Nikic, T. Plass, O. Schraidt, J. Szymanski, J. A. Briggs, C. Schultz, E. A. Lemke, *Angew. Chem. Int. Ed.* **2014**, *53*, 2245-2249.
- [3] X. Chen, Y.-W. Wu, *Org. Biomol. Chem.* **2016**, *14*, 5417-5439.
- [4] a) J. Porath, J. A. N. Carlsson, I. Olsson, G. Beltrage, *Nature* **1975**, *258*, 598-599; b) E. Hochuli, H. Döbeli, A. Schacher, *J. Chrom. A* **1987**, *411*, 177-184.
- [5] a) A. N. Kapanidis, Y. W. Ebricht, R. H. Ebricht, *J. Am. Chem. Soc.* **2001**, *123*, 12123-12125; b) E. G. Guignat, R. Hovius, H. Vogel, *Nat. Biotechnol.* **2004**, *22*, 440-444.
- [6] S. Lata, A. Reichel, R. Brock, R. Tampe, J. Piehler, *J. Am. Chem. Soc.* **2005**, *127*, 10205-10215.
- [7] a) A. Tinazli, J. Tang, R. Valiokas, S. Picuric, S. Lata, J. Piehler, B. Liedberg, R. Tampé, *Chemistry* **2005**, *11*, 5249-5259; b) A. Kollmannsperger, A. Sharei, A. Raulf, M. Heilemann, R. Langer, K. F. Jensen, R. Wieneke, R. Tampe, *Nat. Commun.* **2016**, *7*, 10372; c) K. Gatterdam, E. F. Joest, M. S. Dietz, M. Heilemann, R. Tampé, *Angew Chem Int Ed Engl* **2018**.
- [8] S. Lata, M. Gavutis, R. Tampe, J. Piehler, *J. Am. Chem. Soc.* **2006**, *128*, 2365-2372.
- [9] V. Roullier, S. Clarke, C. You, F. Pinaud, G. G. Gouzer, D. Schaible, V. Marchi-Artzner, J. Piehler, M. Dahan, *Nano. Lett.* **2009**, *9*, 1228-1234.
- [10] A. Reichel, D. Schaible, N. Al Furokh, M. Cohen, G. Schreiber, J. Piehler, *Anal. Chem.* **2007**, *79*, 8590-8600.
- [11] a) C. L. van Broekhoven, J. G. Altin, *Biochim. Biophys. Acta* **2005**, *1716*, 104-116; b) S. Lata, M. Gavutis, J. Piehler, *J. Am. Chem. Soc.* **2006**, *128*, 6-7.
- [12] V. Platt, Z. Huang, L. Cao, M. Tiffany, K. Riviere, F. C. Szoka, Jr., *Bioconjug. Chem.* **2010**, *21*, 892-902.
- [13] S. Lata, J. Piehler, *Anal. Chem.* **2005**, *77*, 1096-1105.
- [14] R. Valiokas, G. Klenkar, A. Tinazli, A. Reichel, R. Tampé, J. Piehler, B. Liedberg, *Langmuir* **2008**, *24*, 4959-4967.
- [15] J. S. Kim, C. A. Valencia, R. Liu, W. Lin, *Bioconjug. Chem.* **2007**, *18*, 333-341.
- [16] M. Braner, A. Kollmannsperger, R. Wieneke, R. Tampé, *Chem. Sci.* **2016**, *7*, 2646-2652.
- [17] R. Wei, V. Gatterdam, R. Wieneke, R. Tampé, U. Rant, *Nat. Nanotechnol.* **2012**, *7*, 257.
- [18] a) G. Giannone, E. Hosity, F. Levet, A. Constals, K. Schulze, A. I. Sobolevsky, M. P. Rosconi, E. Gouaux, R. Tampe, D. Choquet, L. Cognet, *Biophys. J.* **2010**, *99*, 1303-1310; b) O. Rossier, V. Oceau, J. B. Sibarita, C. Leduc, B. Tessier, D. Nair, V. Gatterdam, O. Destaing, C. Albiges-Rizo, R. Tampe, L. Cognet, D. Choquet, B. Lounis, G. Giannone, *Nat. Cell Biol.* **2012**, *14*, 1057-1067.
- [19] a) R. Wombacher, M. Heidebreder, S. van de Linde, M. P. Sheetz, M. Heilemann, V. W. Cornish, M. Sauer, *Nat. Methods* **2010**, *7*, 717-719; b) R. Wieneke, A. Raulf, A. Kollmannsperger, M. Heilemann, R. Tampe, *Angew. Chem. Int. Ed.* **2015**, *54*, 10216-10219.
- [20] Z. Huang, P. Hwang, D. S. Watson, L. Cao, F. C. Szoka, Jr., *Bioconjug. Chem.* **2009**, *20*, 1667-1672.
- [21] A. E. Backmark, N. Olivier, A. Snijder, E. Gordon, N. Dekker, A. D. Ferguson, *Protein Sci.* **2013**, *22*, 1124-1132.
- [22] D. J. O'Shannessy, M. Brigham-Burke, K. K. Sonesson, P. Hensley, I. Brooks, *Anal. Biochem.* **1993**, *212*, 457-468.
- [23] K. N. Richter, N. H. Revelo, K. J. Seitz, M. S. Helm, D. Sarkar, R. S. Saleeb, E. D'Este, E. Eberle, E. Wagner, C. Vogl, D. F. Lazaro, F. Richter, J. Coy-Vergara, G. Coceano, E. S. Boyden, R. R. Duncan, S. W. Hell, M. A. Lauterbach, S. E. Lehnart, T. Moser, T. F. Outeiro, P. Rehling, B. Schwappach, I. Testa, B. Zapiec, S. O. Rizzoli, *EMBO J* **2018**, *37*, 139-159.
- [24] A. Kollmannsperger, A. Sharei, A. Raulf, M. Heilemann, R. Langer, K. F. Jensen, R. Wieneke, R. Tampé, *Nat Commun* **2016**, *7*, 10372.

## COMMUNICATION

## COMMUNICATION

**And the winner is:  
cyclic trisNTA**

The scaffold design controls the interaction of minimalistic trivalent NTA chelators for in-vitro and in-cell labeling of His-tagged proteins.



Karl Gatterdam, Eike F. Joest, Volker Gatterdam, and Robert Tampé\*

Page No. – Page No.

**Scaffold design of trivalent chelator heads dictates high-affinity and stable His-tagged protein labeling *in vitro* and *in cellulo***